

Gauss procedure for the construction of self-localized solitons in discrete systems

R. Dusi and M. Wagner

Institut für Theoretische Physik III, Universität Stuttgart, Pfaffenwaldring 57, 70550 Stuttgart, Germany

(Received 27 February 1995)

Recently, stable self-localized solitons (SLS) have been found in the Fermi-Pasta-Ulam (FPU) chain. In the present investigation a construction procedure for SLS solutions is presented. It is based on two ingredients: (a) the exploitation of the harmonic wing property, and (b) a Gaussian step-by-step optimization starting from the wing. The procedure allows for highly accurate approximate solutions, which already surpass in the one-frequency version the accuracy of previous solutions. The method is illustrated for the quartic FPU chain, but it is not restricted to this type of anharmonicity.

I. INTRODUCTION

The literature on solitary solutions in nonlinear continuous media is very rich. By contrast, in the field of discrete lattices up to now only one exactly solvable system has been found. For this system, which is characterized by an interaction potential of the form $V(x) = (a/b)e^{-bx} + ax$; ($a, b > 0$), Toda has found propagating solitary solutions of the classical equation of motion,¹ with a velocity bigger than the sound velocity. Numerical simulations seem to indicate, however, that no self-localized excitations are possible in the Toda chain.

Historically, the first anharmonic system of discrete nature is the Fermi-Pasta-Ulam chain (FPU chain). In a famous investigation,² Fermi, Pasta, and Ulam have studied numerically the problem of the equipartition of energy in a one-dimensional anharmonic lattice. In fact the FPU system has kept its fascination up to the present, and also in this system propagating solitons have been found.³⁻⁵

Recently Sievers and Takeno⁶ have proposed the existence of a kind of localized mode (self-localized soliton, SLS) in the FPU lattice with an harmonic and an additional hard quartic potential. The existence of the SLS in the FPU chain has been confirmed by molecular-dynamics simulations^{7,8} and in recent works⁹⁻¹³ the properties of these modes are investigated. In our previous work,^{14,15} our emphasis has been on the evolutionary process of local excitations of the FPU chain of alternative prototypes. Specifically, three alternative types of local stimulation have been handled by means of direct molecular-dynamics simulation: (a) an initial displacement of the particle at site $n=0$, (b) an initial impulse at the same site, and finally (c) a force acting on site $n=0$ for a given time period. From these studies it has turned out that the characteristic features of the evolution crucially depend on the type of initial stimulation. E.g., for an impulse excitation the main outcome is a pair of supersonic "compressive" propagating solitons, if the excitation energy is small, whereas for high energies additional supersonic solitons both of "rarefactive" and compressive nature and also subsonic solitons may be generated. By contrast, a single-site local displacement excitation does not display propagating solitons in regular chains.

Rather, in the long-time limit, it displays a stable self-localized mode of the Sievers-Takeno type, provided the energy is not too large. For higher energies the single SLS eventually splits up in several spatially separated SLS modes.

The SLS's are reminiscent of localized vibrations present in a harmonic lattice containing point defects, but the main difference is that in translationally invariant FPU lattices they can occur at any lattice site. The existence of these modes is not limited to one-dimensional lattices but they can also exist in two-dimensional or three-dimensional lattices under certain conditions.¹⁶

In this paper we present a numerical procedure which allows the accurate calculation of the form and of the frequencies of the SLS in the FPU chain. The extension to other types of anharmonicity is straightforward. The procedure is based on the knowledge of the solution in the wing region and on a recursive minimization of a Gaussian error integral concerning the equation of motion. Our numerical results are compared with other approximate solutions,^{12,9} and an analysis of the quality of the solutions will be given by means of the mean-square variance of integrals of motion (energy and momentum).

This paper is organized as follows. In Sec. II we present the model and in Sec. III the numerical procedure. The comparison with other analytical solutions is discussed in Sec. IV and the analysis of the stability of the solutions is given in Sec. V. Finally in Sec. VI we present a summary and discussion.

II. THE MODEL

We consider a regular one-dimensional chain (FPU chain) with nearest-neighbor harmonic and anharmonic interaction described by the Hamilton function:

$$\mathcal{H} = \sum_n \left\{ \frac{p_n^2}{2m} + \sum_{n'=n\pm 1} \left[\frac{f_2}{4} (q_n - q_{n'})^2 + \frac{f_4}{8} (q_n - q_{n'})^4 \right] \right\}, \quad (1)$$

where q_n and p_n are the displacement and momentum of

the n th atom, f_2 and f_4 are, respectively, the harmonic and anharmonic force constants and m is the mass of the atoms. For the harmonic chain ($f_4=0$) the maximal phonon frequency is given by

$$\omega_D = 2\sqrt{f_2/m} . \quad (2)$$

Let a be an arbitrary reference amplitude. Then we may introduce dimensionless variables:

$$Q_n = \frac{q_n}{a}, \quad P_n = \frac{p_n}{(m\omega_D a)}, \quad \tau = \omega_D t . \quad (3)$$

The Hamiltonian equations of motion then read

$$\begin{aligned} \frac{d}{d\tau} Q_n &= P_n , \\ \frac{d}{d\tau} P_n &= -\frac{1}{4} \sum_{n'=n\pm 1} [(Q_n - Q_{n'}) + K(Q_n - Q_{n'})^3] , \end{aligned} \quad (4)$$

where $K = f_4 a^2 / f_2$. The Hamiltonian in our dimensionless variables is given by

$$\mathcal{H} = (ma^2\omega_D^2) \sum_n H_n , \quad (5)$$

where

$$\begin{aligned} H_n &= \frac{1}{2} \left[\frac{dQ_n}{d\tau} \right]^2 \\ &+ \frac{1}{16} \sum_{n'=n\pm 1} \left[(Q_n - Q_{n'})^2 + \frac{K}{2} (Q_n - Q_{n'})^4 \right] \end{aligned} \quad (6)$$

is the dimensionless energy per lattice site. For convenience we always will choose $K=1$, which is no restriction of generality but is to be considered as a choice of the arbitrary amplitude-dimension parameter a .

III. THE METHOD

Recent theoretical and numerical studies^{6,9,12,10,7,8} have demonstrated that spatially localized oscillations (self-localized solitons) can exist in a lattice with quartic anharmonicity. The main characteristics of these SLS are an ultra-Debye frequency, antiphase elongations of neighboring atoms and an exponential spatial decrease of the wings.

In this section we describe a procedure apt to find approximate solutions of the equations of motion (4) which describe these SLS. We consider a trial ansatz for the functions $Q_n(\tau)$ and we calculate the integral

$$I(n) = \frac{1}{T} \int_0^T \left[\frac{d^2 Q_n(\tau)}{d\tau^2} - F_n(\tau) \right]^2 d\tau , \quad (7)$$

where

$$F_n(\tau) = -\frac{1}{4} \sum_{n'=n\pm 1} [(Q_n - Q_{n'}) + K(Q_n - Q_{n'})^3] \quad (8)$$

is the force which acts on the n th atom and T is the period of the functions $Q_n(\tau)$. This integral constitutes a Gaussian error integral and is equal to zero if the ansatz for $Q_n(\tau)$ corresponds to the exact solution of the equa-

tion of motion. If we consider an ansatz for $Q_n(\tau)$ which depend on one or more parameters ($\alpha_1, \alpha_2, \dots, \alpha_N$), we can minimize the value of $I(n)$ solving the equations

$$\left[\frac{\partial I(n)}{\partial \alpha_i} \right] = 0, \quad i = 1 \dots N . \quad (9)$$

In this way we obtain the best solution for the given ansatz.

At this point we do not discuss refinements of this variational principle, which in the future may be adopted in the spirit of the original Gaussian principle of classical mechanics.¹⁷ In particular we do not touch upon the problem of auxiliary conditions, which may be adequate to avoid the trivial solution $Q_n(\tau) \equiv 0$, since for our construction principle this is irrelevant.

Since for any prospective localized solution the amplitude Q_n in the wing necessarily turns small, we may neglect the anharmonic part of the equation of motion for great distances from the center of the SLS:

$$\frac{d^2}{d\tau^2} Q_n = -\frac{1}{4} [2Q_n - Q_{n+1} - Q_{n-1}] . \quad (10)$$

For this harmonic equation we consider the ansatz

$$Q_n(\tau) = B e^{-\mu|n|} (-1)^n \cos(\Omega\tau) , \quad (11)$$

where $\Omega = \omega/\omega_D$ is the dimensionless frequency and μ is a real parameter that describes the exponential decay of the wing. This ansatz satisfies Eq. (10) under the condition (wing condition):

$$\Omega = \cosh(\mu/2) . \quad (12)$$

Since this condition, being independent on n must be satisfied for $|n| \rightarrow \infty$, it constitutes a necessary requirement between the intrinsic parameters μ and Ω of the ansatz, which has to be adopted in the anharmonic regime.

For a fixed wing parameter μ we search an approximate solution of the equation of motion (4) in the form

$$Q_n(\tau) = (-1)^n A_n \cos(\Omega\tau) , \quad (13)$$

where Ω is given by Eq. (12). The Gaussian error integral (7) then reads

$$\begin{aligned} I(n) &= \frac{1}{T} \int_0^T \left\{ \left[\left[-\Omega^2 + \frac{1}{2} \right] A_n \right. \right. \\ &\quad \left. \left. + \frac{1}{4} (A_{n+1} + A_{n-1}) \right] \cos(\Omega\tau) \right. \\ &\quad \left. + \frac{K}{4} [(A_n + A_{n+1})^3 \right. \\ &\quad \left. + (A_n + A_{n-1})^3] \cos(\Omega\tau)^3 \right\}^2 d\tau , \end{aligned} \quad (14)$$

where $T = 2\pi/\Omega$. Solving this integral we obtain

$$I(n) = \frac{1}{2} U(n)^2 + \frac{3}{4} U(n)V(n) + \frac{5}{16} V(n)^2 , \quad (15)$$

where

$$U(n) = [(-\Omega^2 + \frac{1}{2}) A_n + \frac{1}{4} (A_{n+1} + A_{n-1})] \quad (16)$$

represents the harmonic part and

$$V(n) = \frac{K}{4} [(A_n + A_{n+1})^3 + (A_n + A_{n-1})^3] \quad (17)$$

the anharmonic one in the Gauss integral.

The main idea of our method is to start the numerical procedure in a spatial region in which the harmonic solution (11) is sufficiently accurate, e.g., in a region on the left side of the soliton and far away from the center such that to the left of a chosen site n_0 the solution is described by the form

$$A_n = B e^{\mu(n-n_0)} \quad \text{for } n \leq n_0. \quad (18)$$

In particular we choose

$$A_{n_0-1} = B e^{-\mu}, \quad (19)$$

$$A_{n_0} = B$$

for two initial sites n_0 and n_0-1 , provided B is sufficiently small. In this procedure we do not yet know the position of the center which depends on the choice of B . It should be noted that a change of B amounts to a translation of the solitary solution. For fixed values of A_{n_0-1} and A_{n_0} the integral $I(n_0)$ is a function of A_{n_0+1} , and we may determine the best value of A_{n_0+1} solving the equation

$$\frac{\partial I(n_0)}{\partial A_{n_0+1}} = 0. \quad (20)$$

If we desire to have an increased accuracy, we have to choose a smaller B value. To be specific about the error made: if we consider the starting situation given in Eq. (19), solving Eq. (20) we obtain

$$A_{n_0+1} = B e^{\mu} + \frac{3}{4} K B^3 [2(1 + e^{\mu})^3 - e^{3\mu} + e^{-3\mu}] + O(B^5), \quad (21)$$

and the deviation from the exponential solution is proportional to B^3 .

Having fixed in this manner the value of A_{n_0+1} , we may proceed in the same manner. Then, the value of A_{n_0} and A_{n_0+1} are used to find A_{n_0+2} solving Eq. (20) with index $n_0 = n_0 + 1$ and so on. . . . This recurrence procedure gives an optimized sequence of A_n values which describe the SLS with a fixed wing parameter μ .

In Fig. 1 we show the quantity A_n as a function of site index n for the wing parameter $\mu = 0.2$ and for two values of the parameter B [see Eq. (19)]. With our approximate numerical procedure the resultant distribution is not exactly symmetric (see Figs. 1 and 2) and also a deviation from the exponential behavior is observed in the right wing. The latter is due to the augmentation of inaccuracies when moving to the right. We now may choose B and n_0 in such a manner that A_0 is a symmetric maximum between its two neighbors ($A_1 = A_{-1}$). After the condition $A_1 = A_{-1}$ is satisfied, the right wing, because of the inaccuracy, still is not symmetric to the left one, whence we replace the amplitude values on the right side

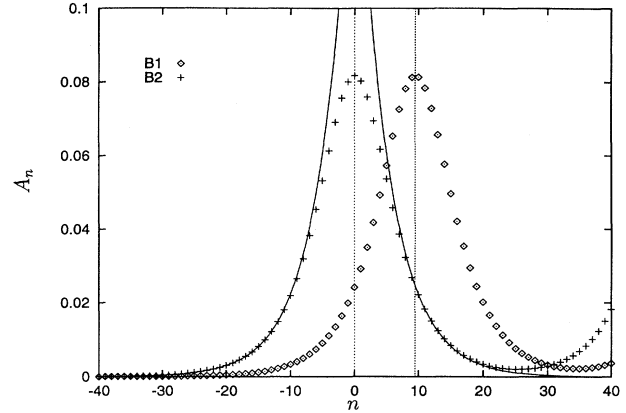


FIG. 1. Maximal displacements A_n as a function of site n for the wing parameter $\mu = 0.2$ and two values of the constant B [see Eq. (19)]. The full line shows the exponential behavior of the harmonic solution $A_n = B e^{\mu|n|}$.

by those of the left side, $A_n = A_{-n}$ for $n > 1$. This is shown in Fig. 6. This solution, if longitudinal motion is considered, constitutes an “odd mode,” which satisfies the condition $Q_n = Q_{-n}$. Vice versa, we may choose B and n_0 in such a manner that $A_1 = A_0$ and replace the amplitudes on the right side in analogous manner by those of the left side, $A_{n+1} = A_{-n}$ for $n > 1$. Then, the longitudinal motions would represent an “even mode” with respect to the site $n = 1/2$, which satisfies the condition $Q_{n+1} = -Q_{-n}$ for $n \geq 0$. In this paper we focus our attention on the odd-symmetry solutions, and the numerical results of our procedure are always understood as being symmetrized in the sense just explained.

IV. COMPARISON WITH OTHER ANALYTICAL SOLUTIONS

In the theoretical work of Sievers and Takeno⁶ and of Bickham and Sievers (BS),⁹ approximate analytical solutions are found, using lattice Green functions and the “rotating-wave” approximation (RWA), where also only

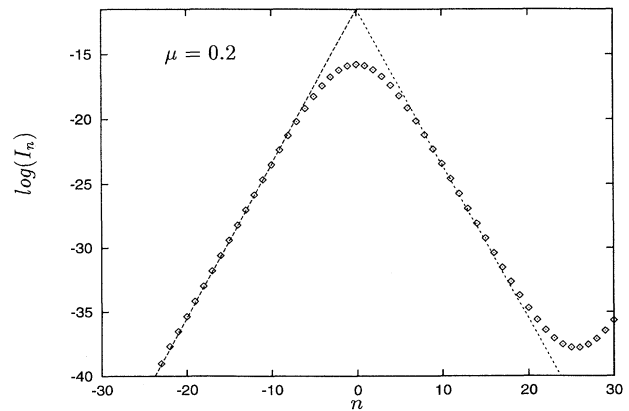


FIG. 2. Logarithm (base 10) of the Gauss integral I_n as a function of site n for the wing parameter $\mu = 0.2$.

a single frequency component is included in the time dependence. With this procedure BS find a solution in the form:

$$\begin{aligned} Q_n(\tau) &= \alpha A_0 (-1)^n e^{-\mu|n|} \cos(\Omega\tau), \\ Q_0(\tau) &= A_0 \cos(\Omega\tau), \end{aligned} \tag{22}$$

where the parameters α, μ, Ω are determined for a fixed "effective anharmonicity parameter" $\gamma_4 = K A_0^2$ by solving a system of equations obtained with the RWA.

At this place it is worth looking back at the original variables. We have defined $K = (f_4/f_2)a^2$ and chosen $K=1$. On the other hand we have $q_0 = a A_0$, whence we find

$$\gamma_4 = f_4/f_2 q_0^2 = A_0^2. \tag{23}$$

Hence, a specific solution (22) which is fixed by taking a specific value of A_0 , can either be reached by a large relative anharmonicity constant f_4/f_2 combined with a small amplitude q_0 or vice versa.

Another analytical solution is given by Yoshimura and Watanabe (YW).¹² In this work the authors derive a nonlinear Schrödinger equation as a continuum approximation of the lattice and find a solution which describes the SLS as an envelope soliton. The solution reads

$$R_n(\tau) = A_0 (-1)^n \text{sech}(\sqrt{3K/2} A_0 n) \cos(\Omega\tau), \tag{24}$$

where $R_n = Q_n - Q_{n-1}$ is the relative displacement, $\Omega = 1 + (3/16)\gamma_4$ and $\gamma_4 = K A_0^2$. This solution displays even symmetry in the Q space and for localized modes ($\lim_{|n| \rightarrow \infty} R_n = 0$) the transformation $R_n \rightarrow Q_n$ is defined by

$$Q_n = \sum_{i=-\infty}^n R_i. \tag{25}$$

For small γ_4 the transformation of Eq. (24) gives the solution

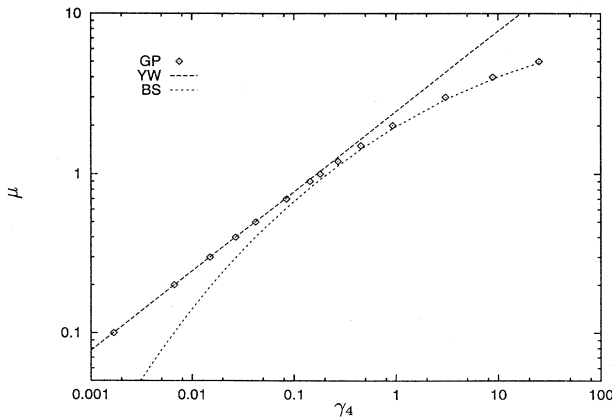


FIG. 3. Wing parameter μ as a function of the anharmonicity parameter γ_4 for our solutions (GP), for the solutions of Bickham and Sievers (BS) and for the solutions of Yoshimura and Watanabe (YW).

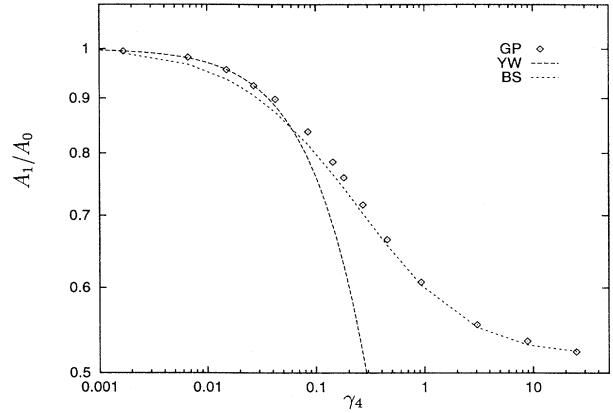


FIG. 4. Ratio A_1/A_0 as a function of the anharmonicity parameter γ_4 for our solutions (GP) and for the solutions of BS and YW.

$$Q_n(\tau) = A_0 (-1)^n \text{sech}[\sqrt{6K A_0^2} (n + 1/2)] \cos(\Omega\tau), \tag{26}$$

which directly evinces the even-symmetry longitudinal motion. The passage from even symmetry to odd symmetry for small values of γ_4 can be considered as a shifting of the form (26) by $\delta_n = 1/2$. The odd-symmetry solution derived from Eq. (26), then reads

$$Q_n(\tau) = A_0 (-1)^n \text{sech}(\sqrt{6K A_0^2} n) \cos(\Omega\tau), \tag{27}$$

where $\Omega = 1 + (3/4)\gamma_4$ and $\gamma_4 = K A_0^2$. This solution in the terminology of YW would amount to an even-symmetry motion in differential space, $R_n = Q_n - Q_{n-1}$. The solution given in Eq. (27) is also obtained by Kovalev, Usatenko, and Chubykalo¹⁸ in the limit of small anharmonicity. In fact there is no contradiction in the appearance of both parity-type solutions [see Eqs. (27) and (26)], as Kovalev, Usatenko, and Chubykalo seem to

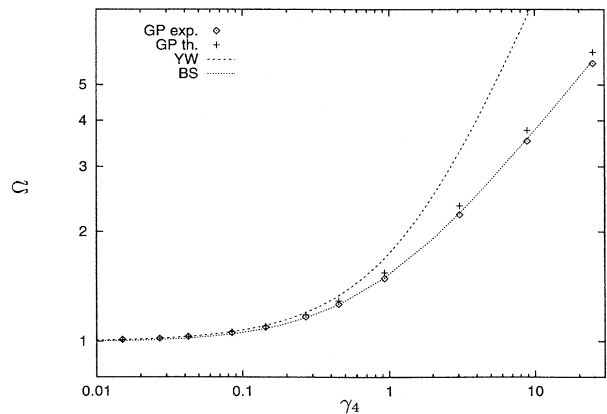


FIG. 5. Frequency Ω of the particle at central site $n=0$ as a function of the anharmonicity γ_4 for our solutions and for the solutions of BS and YW. "GP exp" indicates the measured frequency of $Q_0(\tau)$ obtained with numerical simulation and "GP th" is the theoretical value of the frequency predicted by the wing condition [see Eq. (12)].

insinuate. In our calculations we have found that for small anharmonicity both types can exist and be stable.

In our numerical procedure the wing parameter μ is taken as a fixed quantity. Then, considering odd solutions, the value of the anharmonicity parameter $\gamma_4 = K A_0^2$ is determined by the maximum value of the displacement A_0 . In Fig. 3 we show the parameter μ as a function of the anharmonicity γ_4 and we observe that for small γ_4 the values of μ for our solutions are in agreement with the solutions of YW. On the other hand, for greater anharmonicity our solutions are in agreement with the solutions of BS. The same behavior is observed also for the quantity A_1/A_0 (see Fig. 4) and for the frequency Ω (see Fig. 5). These results show that our solutions connect the solutions of YW for $\gamma_4 \ll 1$ with the solutions of BS for $\gamma_4 \gg 1$. As noted, the BS solution is very good for $\gamma_4 \gg 1$. In fact Figs. 4 and 5 even seem to indicate that the solutions of BS also in the small γ_4 limit are rather accurate. But later it will turn out otherwise (see below).

In Fig. 6 we show the absolute value of the displacement A_n as a function of the site index n for a small anharmonicity. In this case we observe that the values of A_n obtained with our numerical procedure are in perfect agreement with the solution of YW. For the same maximum amplitude A_0 the solution of BS displays a less steep wing, i.e., a smaller wing parameter μ and there is also a considerable deviation in the central region. The solutions of YW are obtained from a continuum approximation of the lattice, whence these solutions are valid only for small anharmonicity. For greater anharmonicity ($\gamma_4 \gg 1$) the vibrational motion involves only a small number of particles and it is reminiscent of the vibrations of a triatomic molecule (see Fig. 7). In this limit the YW solution practically would involve only a single particle and the resultant total momentum of the chain would not be conserved. On the other hand the solution given by BS exhibits a displacement pattern (. . ., 0, -0.52, 1, -0.52, 0, . . .) which is normalized to the central amplitude A_0 and which is in agreement with our numerical solution for the three central particles. How-

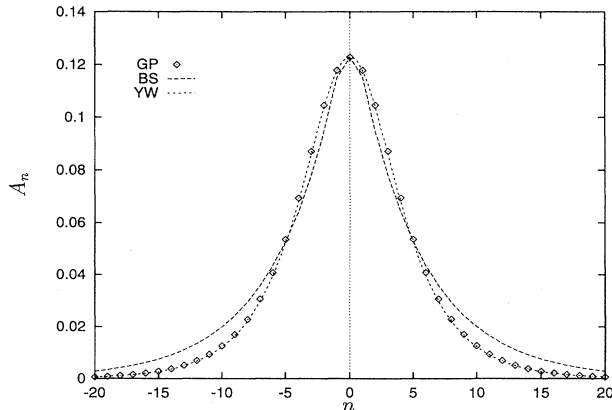


FIG. 6. Maximal displacements A_n as a function of site n for our solution (GP) and for the BS and YW solution. The value of the anharmonicity is $\gamma_4 = 0.015$.

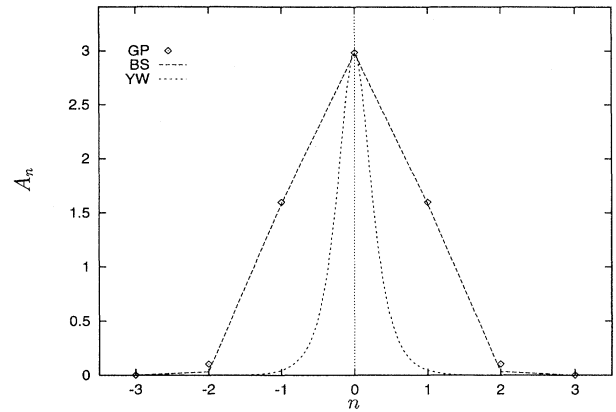


FIG. 7. Maximal displacements A_n as a function of site n for our solution (GP) and for the BS and YW solution. The value of the anharmonicity is $\gamma_4 = 8.8$.

ever our solution shows a considerable greater value of A_2 . In a recent work, Sandusky, Page, and Schmidt¹¹ have investigated a chain with purely quartic anharmonicity. In this case the odd-symmetry mode has a fixed normalized displacement pattern given by (. . ., 0, 0.02, -0.52, 1, -0.52, 0.02, 0, . . .) which is very close to our solution in the strong anharmonicity regime. In this limit ($\gamma_4 \gg 1$) the equation of motion is dominated by the linear term and we expect that the displacement pattern given by Sandusky, Page, and Schmidt is correct also for the FPU chain with quartic anharmonicity. This question is investigated in the next section where the stability of solutions is verified with numerical simulations.

A possible way to characterize the accuracy of approximate solutions in a global way is by means of integrals of motion. If C_α is a conserved quantity, we may consider the mean-square variance

$$\langle C_\alpha^2 \rangle - \langle C_\alpha \rangle^2 \quad (28)$$

of this quantity relating to the approximate solution. In our case the total momentum

$$P = \sum_n P_n \quad (29)$$

is a conserved quantity and we define

$$\langle P \rangle = \frac{1}{T} \int_0^T \sum_n P_n(\tau) d\tau; \quad (30)$$

and

$$\langle P^2 \rangle = \frac{1}{T} \int_0^T \left[\sum_n P_n(\tau) \right]^2 d\tau; \quad (31)$$

For even (longitudinal) modes $\langle P^2 \rangle = 0$ by symmetry. But since we want to consider odd modes, the mean-square variance of P is a nontrivial characterization. In Fig. 8 we present the mean-square momentum fluctuation as a function of the mean energy,

$$\langle H \rangle = \frac{1}{T} \int_0^T \sum_n H_n(\tau) d\tau \quad (32)$$

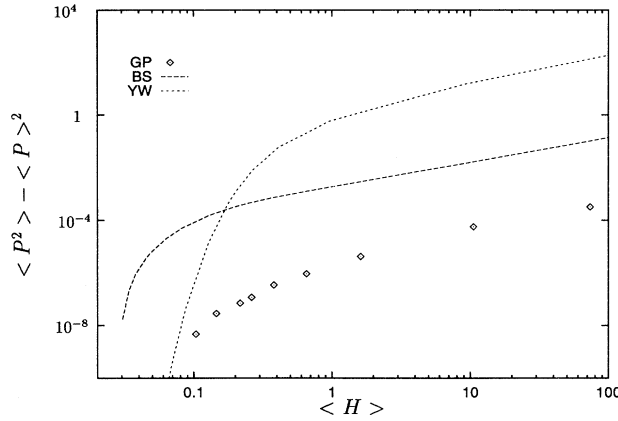


FIG. 8. Mean-square variance of the total momentum as a function of the mean total energy for our solutions (GP) and for the solutions of YW and BS.

for odd modes.

For $\langle H \rangle > 0.1$ we note a smooth behavior of the curve pertaining to our numerical procedure. It always lies below the results of YW and BS and for $\langle H \rangle > 1$ is at least two orders of magnitude lower than both other results. For small values of $\langle H \rangle$ ($\langle H \rangle < 0.1$) our result can be shown to merge analytically into that of YW. This can be seen as follows. We consider the value of the amplitude given by the YW solution [Eq. (27)]

$$A_{n-1} = A_{n-1}^{\text{YW}} = \frac{A_0}{\cosh[\mu(n-1)]}, \quad (33)$$

$$A_n = A_n^{\text{YW}} = \frac{A_0}{\cosh(\mu n)},$$

and we search for the optimized value of A_{n+1} solving Eq. (20). Let $A_{n+1} = A_{n+1}^{\text{YW}} + X_{n+1}$ we obtain in the limit $\langle H \rangle \rightarrow 0$ (which corresponds to $\mu \rightarrow 0$)

$$X_{n+1} \propto \mu^4 A_{n+1}^{\text{YW}}. \quad (34)$$

From this expression we obtain

$$P_n^{\text{GP}} = P_n^{\text{YW}} [1 + O(\mu^4)], \quad (35)$$

where the index GP (Gauss procedure) indicate our numerical solution. The mean-square variance of the momentum is given by

$$\langle P^2 \rangle^{\text{GP}} = \langle P^2 \rangle^{\text{YW}} [1 + O(\mu^4)], \quad (36)$$

and for $\mu \rightarrow 0$ we obtain $\langle P^2 \rangle^{\text{GP}} \rightarrow \langle P^2 \rangle^{\text{YW}}$. It should be noted, however, that any “test solution” which displays a small value of the quantity (28) not necessarily indicates an approach to the exact solution; the requirement of small fluctuation may also be satisfied by functional forms which strongly violate the equation of motion. An illustration of this point is noted if the relative fluctuation of the total energy, $(\langle H^2 \rangle - \langle H \rangle^2) / \langle H \rangle^2$, is considered (see Fig. 9). Here we define

$$\langle H^2 \rangle = \frac{1}{T} \int_0^T \left[\sum_n H_n(\tau) \right]^2 d\tau. \quad (37)$$

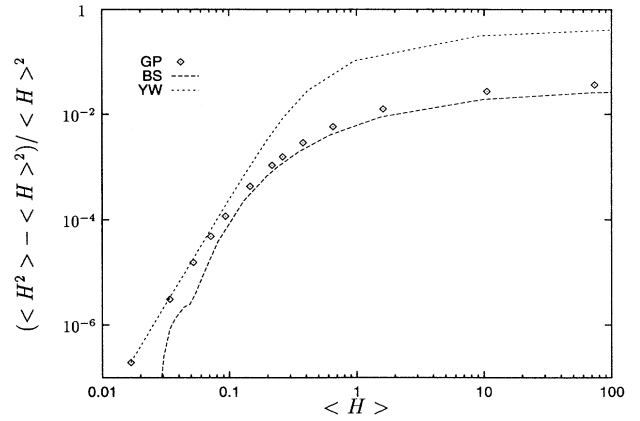


FIG. 9. Relative mean-square variance of the total energy as a function of the mean total energy for our solutions (GP) and for the solutions of YW and BS.

In Fig. 9 we note that for small $\langle H \rangle$ values the BS form yields the smallest relative energy fluctuation, although we know (see, for example, Fig. 6) that in this regime both the solutions of YW and of our numerical procedure satisfy the equation of motion much better. On the other hand, for large $\langle H \rangle$ values we find a relative energy fluctuation which is close to the BS solution. For the stationarity of the solutions in this energy regime we refer to the next section.

V. STABILITY OF THE SOLUTIONS

All solutions considered so far have a time behavior $Q_n(\tau) \propto \cos(\Omega\tau)$, whence $P_n(0) = 0$. Using now the found amplitude distribution of each solution at $\tau = 0$ [$Q_n(0) = (-1)^n A_n$; $P_n(0) = 0$], we can follow up the time evolution by numerically solving the equation of motion (4). We do that by a fourth-order Runge-Kutta method. The time step in our program is always chosen to preserve the total energy of the lattice to an accuracy better than 10^{-4} . For each considered initial condition we have an exponential decrease of the wings and we start with a chain of a length such that all neglected sites have an amplitude $A_n < 10^{-10}$ at time $\tau = 0$. This choice is made, since taking a longer chain, no change in the behavior is noted any more. The chain is treated in a self-expanding manner,¹⁹ i.e., we expand it whenever the energy on the last atoms exceeds a preset small value. With this artifice the chain is effectively infinite.

For small effective anharmonicity ($\gamma_4 = 0.015$) we have considered the initial conditions given in Fig. 6. In this case, our numerical solution corresponds to the YW solution whereas the BS solution deviates somewhat.

In Fig. 10 we show the value of $\sum_{n=25}^{\infty} H_n / \sum_{n=-\infty}^{\infty} H_n$ as a function of the time τ . This quantity measures the removal of the energy from the center and is indicative for the stability of the solution. We observe that for the initial condition of BS, this quantity has a large increase at small times but then shows the tendency to reach a constant value. At the end of this process a fraction of about 2×10^{-3} of the total energy is

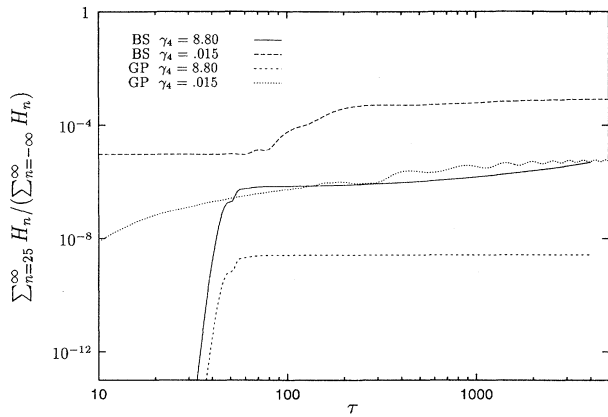


FIG. 10. $\sum_{n=25}^{\infty} H_n / \sum_{n=-\infty}^{\infty} H_n$ as a function of the time τ obtained for our (GP) initial conditions [$Q_n(0) = (-1)^n A_n$; $P_n(0) = 0$] and for the initial conditions of BS. The values of the anharmonicity considered are $\gamma_4 = 0.015$ and $\gamma_4 = 8.8$ (see Figs. 6 and 7).

transformed in energy packets which propagate away from the center whereas the central region now is stable. Taking the solution of our procedure as the initial conditions the process of stabilization takes away only $\approx 10^{-5}$ of the total energy. Another aspect of the process of stabilization is displayed in Fig. 11 where we show the maximal value $Q_0^{\max}(\tau)$ of the wave amplitude at the center of the soliton as a function of the time τ . For the initial condition of BS we observe an oscillatory behavior and the value of Q_0^{\max} shows the tendency to research a constant value smaller than the initial one. On the other hand, we observe that for an initial condition pertaining to our procedure the value of Q_0^{\max} remains approximately constant. For small anharmonicity the soliton form given by BS is not stable and after a sufficiently large time (1000 periods), it transforms into the YW form with a

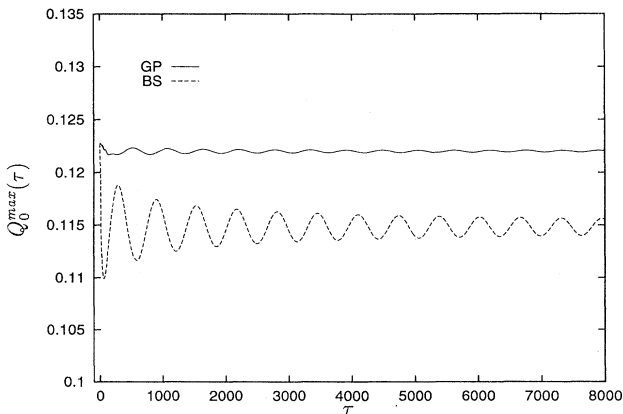


FIG. 11. Maximal value of the wave amplitude at site $n=0$ as a function of time τ as obtained for our initial condition (GP) and for the initial condition of BS [$Q_n(0) = (-1)^n A_n$; $P_n(0) = 0$] displayed in Fig. 6 ($\gamma_4 = 0.015$).

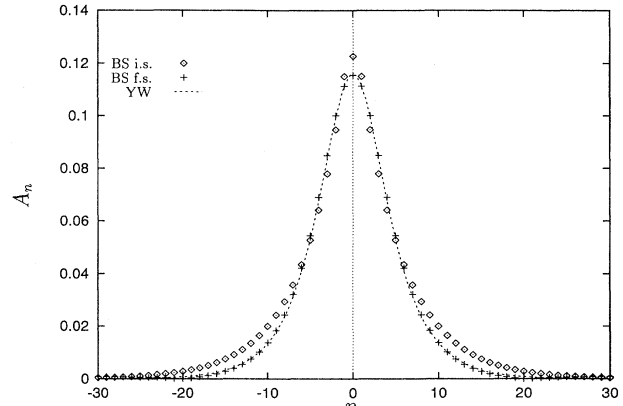


FIG. 12. Maximal displacements A_n as a function of the site index n . The points (BS i.s.) represent a BS-initial state calculated for the anharmonicity parameter $\gamma_4 = 0.015$, i.e., $Q_n(0) = (-1)^n A_n$; $P_n(0) = 0$ and the crosses (notation BS f.s.) indicate the values of A_n at time $\tau = 8000$. The line YW shows the analytical solution of Yoshimura and Watanabe with anharmonicity $\gamma_4 = K A_0^2$ adapted to the amplitude A_0 of the final condition.

smaller value of γ_4 (see Fig. 12). These numerical experiments confirm that for small anharmonicity the amplitude distribution of our procedure (which correspond to the YW solutions at the time $\tau = 0$) remains stable.

For greater values of the anharmonicity ($\gamma_4 = 8.8$) our solutions are similar to the BS solutions. In the molecular-dynamics experiments we have considered the initial conditions given in Fig. 7. Figure 13 shows the time evolutions of $Q_0^{\max}(\tau)$. Here the BS initial condition yields an oscillatory behavior which does not disappear for a long time, whereas the initial conditions pertaining to our procedure display a much smaller fluctuation and is stable, as seen in Fig. 10. The portion of the energy that propagates away from the center (see Fig. 10) indicates that the initial conditions of BS generate an unsta-

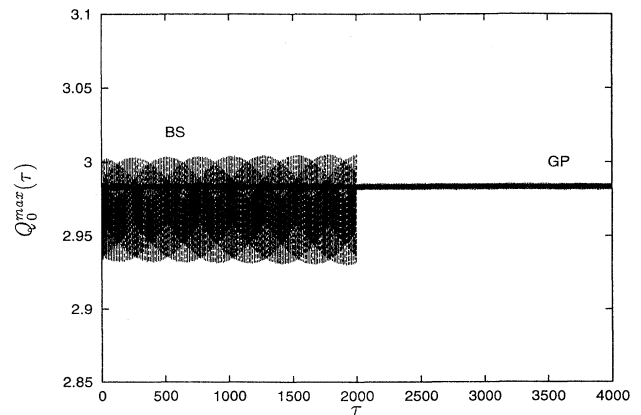


FIG. 13. Maximal value of the wave amplitude at site $n=0$ as a function of the time τ obtained for our initial condition (GP; $0 < \tau < 4000$) and for the initial condition of BS ($0 < \tau < 2000$; $Q_n(0) = (-1)^n A_n$; $P_n(0) = 0$ displayed in Fig. 7 ($\gamma_4 = 8.8$).

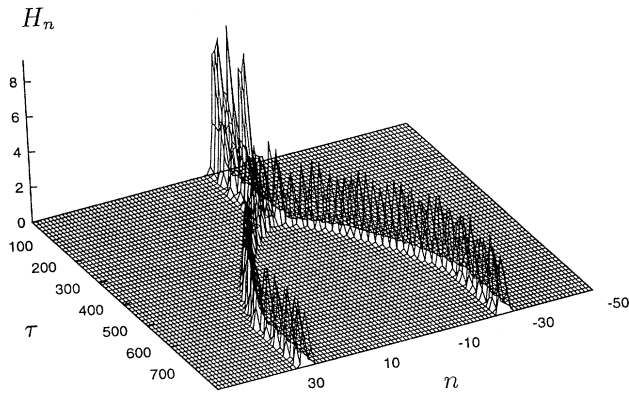


FIG. 14. Spatiotemporal evolution of the site energy $H_n(\tau)$ for the initial condition [$Q_n(0)=(-1)^n A_n$; $P_n(0)=0$] of YW with anharmonicity $\gamma_4=8.8$ (see Fig. 7).

ble mode, whereas for our initial conditions the mode reaches a stationary state after an initial time of ≈ 20 periods and only a fraction of about 10^{-8} of the total energy spreads out. The evolution for the initial conditions of YW is very different and displays a bifurcation in space (see Fig. 14). In Fig. 14 we note that after some time has passed the energy packet splits up in two localized solitons with a smaller effective anharmonicity parameter. Further numerical experiments for greater values of γ_4 as well as for intermediate values demonstrate the stability of an evolution following initial conditions generated by our procedure.

An interesting phenomenon is observed in Fig. 5. If we take our numerically found form as the initial condition [$Q_n(0)=(-1)^n A_n$; $P_n(0)=0$], the simulation (=“experiment”) yields for the particle at site $n=0$ a measured frequency Ω , which for great anharmonicity is somewhat smaller than the theoretical one [see Eq. (12)]. To explain this we must note that for great values of the wing parameter μ (large anharmonicity) a small change of the wing parameter μ causes a relatively great change of the frequency Ω :

$$\Delta\Omega \approx \left(\frac{d\Omega}{d\mu} \right) \Delta\mu = \frac{1}{2} \sinh \left(\frac{\mu}{2} \right) \Delta\mu. \quad (38)$$

We should, however, note that these deviations of Ω take place in an anharmonicity regime which hardly can be realized in nature. We may expect that during the evolution the wing of our initial form changes somewhat, preserving only the stable part with an effective wing parameter μ smaller than the initial one.

VI. SUMMARY AND DISCUSSION

In this investigation we present a procedure for the calculation of a self-localized soliton in chains with anharmonic nearest-neighbor potentials, which exploits the known limiting behavior of the spatial wings. The crucial idea is that for localized solutions, the solution in the

wing region must merge into a solution of the harmonic chain, i.e., into the form

$$A_n \propto e^{-\mu|n|} (-1)^n \quad \text{for } |n| \rightarrow \infty. \quad (39)$$

The knowledge of the form in the wing region is used as starting condition in our procedure (“construction out of the wing”). Our method is based on a step by step minimization of the Gaussian error integral [see Eq. (7)] and for a given wing parameter μ we can construct the complete form of the SLS by a recursive procedure. This method furnishes even-symmetry or odd-symmetry solutions, but in this paper we have considered only odd-symmetry solutions. Our procedure can be applied to any type of anharmonicity, but for illustrative purposes we consider the quartic Fermi-Pasta-Ulam chain, which historically is the most fascinating one, and which has been considered by many other investigators.

The approximate solutions obtained with our procedure are compared with the solutions given by Bickham and Sievers⁹ and by Yoshimura and Watanabe.¹² We show that for small energy our solution merges into the solution given by YW. On the other hand, for great energy our procedure gives a solution which is in good agreement with the solutions of BS. For extremely high values of the energy we find that our solution involves practically only three particles and merges into the solution given by Sandusky, Page, and Schmidt¹¹ for a purely anharmonic lattice. To test the validity of the solutions the mean-square variance of the integrals of motion (energy and momentum) is used. The analysis shows that our procedure gives good solutions for all energy regimes, which is not true for other approximate analytical solutions (BS and YW). The accuracy of the various solutions is also tested with numerical simulations of the time evolution. We show that the initial conditions pertaining to our procedure generate stable modes, maintaining the initial form. By contrast, if we consider the initial condition pertaining to the BS or YW solutions, we find that the evolution is not stable for respectively unsuitable energy regions. For example the YW initial condition for great energy displays a bifurcation in space and the BS initial condition for small energy shows an unstable behavior, resulting in a modification of the wing parameter μ .

Our numerical procedure is only an optimized approximation of the exact solution. Its accuracy depends on the chosen functional form and may be improved both in the choice of the starting wing amplitudes as in the choice of the time behaviors. For example, numerical simulations and theoretical works^{13,9} have demonstrated that the exact solution of the equation of motion contains higher frequencies which are odd multiples of the fundamental frequency Ω . However, the amplitude of these higher-frequency additions are small fractions of the amplitude at the fundamental frequency, and in the present illustration they are ignored. Therefore with the chosen ansatz [see Eq. (13)], it is not possible to make the Gauss-integral equal to zero, $I(n)=0$, and the minimum values of $I(n)$ can be interpreted as a measure of the goodness of the approximate solution.

- ¹M. Toda, J. Phys. Soc. Jpn. **22**, 431 (1967).
²E. Fermi, J. R. Pasta, and S. M. Ulam, *E-Fermi*, Collected Papers (Univ. of Chicago Press, Chicago, 1965), Vol. II, p. 978.
³N. J. Zabusky, Comput. Phys. Commun. **50**, 1 (1973).
⁴M. Peyrard, St. Pnevmatikos, and N. Flytzanis, Physica D **19**, 268 (1986).
⁵G. S. Zavt, M. Wagner, and A. Luetze, Phys. Rev. E **47**, 4108 (1993).
⁶A. J. Sievers and T. Takeno, Phys. Rev. Lett. **61**, 970 (1988).
⁷R. Bourbonnais and R. Maynard, Phys. Rev. Lett. **64**, 1397 (1990).
⁸V. M. Burlakov, S. A. Kiselev, and V. N. Pyrkov, Solid State Commun. **74**, 327 (1990).
⁹S. R. Bickham and A. J. Sievers, Phys. Rev. B **43**, 2339 (1991).
¹⁰J. B. Page, Phys. Rev. B **41**, 7835 (1990).
¹¹K. W. Sandusky, J. B. Page, and K. E. Schmidt, Phys. Rev. B **46**, 6161 (1992).
¹²K. Yoshimura and S. Watanabe, J. Phys. Soc. Jpn. **60**, 82 (1991).
¹³S. A. Kiselev, S. R. Bickham, and A. J. Sievers, Phys. Rev. B **48**, 13 508 (1993).
¹⁴R. Dusi, G. Viliiani, and M. Wagner, Philos. Mag. B (to be published).
¹⁵R. Dusi, A. Lütze, G. Viliiani, and G. S. Zavt, Philos. Mag. B (to be published).
¹⁶S. Takeno, J. Phys. Soc. Jpn. **59**, 1571 (1990).
¹⁷C. F. Gauss, Crelle's Journal **IV**, 232 (1829), see also "Werke", p. 23.
¹⁸A. S. Kovalev, O. V. Usatenko, and O. A. Chubykalo, Phys. Solid State **35**, 356 (1993).
¹⁹D. Dunlap, K. Kundu, and P. Phillips, Phys. Rev. B **40**, 10 999 (1989).